文章编号:0253-2778(2017)12-1037-07

Effect of post-annealing on the structure and dielectric property of $La_2Ti_2O_7$ thin film

SHAO Tao, WANG Yuyin, LI Yuanyuan, YANG Mei, HU Chuansheng, QI Zeming

(*National Synchrotron Radiation Laboratory, University of Science and Technology of China, Hefei* 230029, *China*)

Abstract: $La_2Ti_2O_7$ thin films were grown on Si (100) substrates by using pulsed laser deposition method. The effect of post-annealing on the structural and dielectric properties of the films at different temperatures was studied by using X-ray diffraction, atomic force microscopy and synchrotron infrared transmission spectroscopy. The results show that the as-deposited thin film is amorphous and annealing thin film is crystallized into monoclinic structure. The infrared spectrum reveals that the annealing can significantly increase the dielectric constant. The as-deposited thin film has a low dielectric constant attributed to the loss of some phonon modes, especially the low frequency mode. This indicates post-annealing has an important influence on the dielectric property of $La_2Ti_2O_7$ thin film.

Key words: high-k gate dielectrics; post-annealing; $La_2Ti_2O_7$ thin film; infrared

CLC number: O482.4 **Document code**: A doi: 10.3969/j.issn.0253-2778.2017.08.010

Citation: SHAO Tao, WANG Yuyin, LI Yuanyuan, et al. Effect of post-annealing on the structure and dielectric property of $La_2Ti_2O_7$ thin film[J]. Journal of University of Science and Technology of China, 2017,47(12):1037-1043.

邵涛,王玉银,李元元,等. 后退火处理对 $La_2Ti_2O_7$ 薄膜结构和介电物理性质的影响[J]. 中国科学技术大学学报,2017,47(12):1037-1043.

后退火处理对 $La_2Ti_2O_7$ 薄膜结构和介电物理性质的影响

邵 涛,王玉银,李元元,杨 梅,胡传圣,戚泽明

(中国科学技术大学国家同步辐射实验室,安徽合肥 230029)

摘要:采用脉冲激光沉积镀膜技术在Si(100)衬底上生长了 $La_2Ti_2O_7$ 栅介质薄膜.通过X射线衍射、原子力显微及同步辐射红外透射光谱技术探索了不同温度下的后退火处理对薄膜结构及介电性能产生的影响.结果表明,未经退火处理的 $La_2Ti_2O_7$ 薄膜为非晶态,退火后薄膜结晶形成单斜结构.红外谱表明退火处理能够显著增加薄膜介电常数.沉积的非晶态薄膜具有较低的介电常数是因为损失了一些声子振动模式,尤其在低波数段损失的更加明显.实验结果说明后退火处理对 $La_2Ti_2O_7$ 薄膜的介电性能有非常重要的影响.

关键词:高介电常数;后退火;$La_2Ti_2O_7$ 薄膜;红外

Received: 2016-05-30; **Revised**: 2016-07-05

Foundation item: Supported by the National Natural Science Foundation of China (11275203, U1732148), National Key Scientific Instrument and Equipment Development Project (2011YQ130018), Technological Development Grant of Hefei Science Center of CAS (2014TDG-HSC002).

Biography: SHAO Tao, male, born in 1987, Master candidate. Research field: dielectric properties of metal oxide thin films. E-mail: shaotao@mail.ustc.edu.cn

Corresponding author: QI Zeming, PhD/Associate Professor. E-mail: zmqi@ustc.edu.cn

0 Introduction

The scaling rule to a metal-oxide-semiconductor field effect transistor (MOSFET) involves a reduction in the thickness of the gate dielectric[1]. However, SiO_2, an effective dielectric, approaches its limit when the thickness of the gate oxide scales below 2nm because of the excessive direct tunneling leakage current and reliability issues[2-4]. To overcome this physical limit, there is a wide range of research being conducted on alternative materials. In previous reports, the usage of high-k dielectrics can increase the physical thickness of gate dielectric to reduce tunneling leakage and improve device reliability [5-7]. Among the high-k gate dielectrics, lanthanum based oxides are currently being studied as high-k materials to substitute SiO_2 in future ultra-large scaled integration devices because they process a combination virtue of high dielectric values, large band gaps and high conduction-band offset on Si[8-9]. Moreover, although TiO_2 films have high permittivity even in amorphous state[10], they cannot be used as high-k gate dielectrics for CMOS devices because of very small conduction band offsets with respect to silicon. La_2O_3, on the other hand, has a large conduction band offset with respect to silicon (~2.3 eV), high permittivity and thermodynamic stability with Si[11]. Although, many low permittivity La_2O_3 films have been reported in the literatures, it is the moisture absorption phenomenon that results in permittivity deterioration and the poor crystalline of La_2O_3 films[12]. Thus, La-based ternary oxides, doped with a second oxide, can have more merits compared with La_2O_3 as high-k gate dielectrics since they exhibit a much stronger moisture resistance than La_2O_3[13-14]. To solve the problem of moisture absorption and poor crystalline, the addition of TiO_2 into rare earth oxide exhibits excellent physical properties such as a thin interfacial layer, a low solubility in water, a high dielectric constant and a low leakage current, because it reduces the reaction of high-k dielectric with water[15-17]. Moreover, the incorporation of TiO_2 or Ti into the lanthanide oxide dielectrics has attracted much attention because of the excellent physical properties of the incorporation the gate insulator for CMOS device application [18-19]. Ti-doped lanthanide oxide films have a much larger band gap than TiO_2 films because of the coupling effect between the La and Ti atoms bonding to the same oxygen atom[20]. Therefore, $La_2Ti_2O_7$ films might be suitable to be used as MOSFET gate dielectrics since a medium conduction band offset with respect to silicon is achieved due to the introduction of La_2O_3. Furthermore, $La_2Ti_2O_7$ thin films can be expected to have high permittivity because of the high permittivity of La_2O_3 and TiO_2. Normally, the as-grown thin film is amorphous, which will affect the infrared phonon modes and cause the static dielectric constant to decrease. The post-annealing is an effective method to improve crystalline quality, thus the main infrared phonon modes are kept and the considerable value of the static dielectric constant can be preserved[21-22].

In this paper, we prepared $La_2Ti_2O_7$ thin film by pulsed laser deposition (PLD) method. The effect of post-annealing on the structure and infrared phonon mode of the thin film was investigated. The structure and infrared phonon information were obtained to thoroughly understand the annealing effect on the dielectric properties of $La_2Ti_2O_7$ thin film.

1 Experimental

$La_2Ti_2O_7$ thin films were grown on n-type Si(100) substrates by pulsed laser deposition method. The target was synthesized using standard solid-state ceramic synthesis methods[19]. The precursor compounds, La_2O_3 (99.99%) and TiO_2 (99. 99%), were weighed in the correct proportions and mixed together. The materials were wet ground in ethanol and then dry ground; both grindings took 20min using an alumina mortar and pestle. The ground powders were pressed into pellets and annealed in three steps. The first two annealing steps were for 12 h at 1000℃ and 1200℃, respectively. The final step was at 1400℃ for 24 h. Between each annealing step, the pellets were re-ground and re-pressed as described above. The $La_2Ti_2O_7$ pellet was then used as the target in the films deposition process.

Prior to deposition, the Si substrate was cleaned via the Radio Corporation of America (RCA) technique to obtain an H-terminated Si surface and treated with a dilute 10% hydrofluoric (HF) for 10s to remove the native oxide. And then the cleaned substrate was set on a heated holder in a PLD chamber. A Lambda Physic LPX200 KrF laser with a wavelength of 248 nm was used for the film deposition. The vacuum of deposition chamber was kept under 2.4×10^{-4} Pa, and Si substrate was heated to 300℃. During the film growth, a KrF excimer laser (248 nm, 5 Hz) was operated and the laser energy was 200 mJ with an energy density of ~2 J/cm^2. The obtained thin films were post annealed in air ambient for 30 s at 900℃, 950℃, 1000℃, respectively.

X-ray diffraction (XRD) analyses were performed using a TTR-III system with a Cu K (λ =1.541841Å) to study the growth directions and crystallization of $La_2Ti_2O_7$ films of as deposited and post-annealed films. Atomic force microscopy (AFM) was used to characterize the surface morphology evolution of the sensing films after annealing at different temperatures, The infrared transmission spectra were measured over 50~700 cm^{-1}, using a Bruker IFS 66v FTIR spectrometer on an infrared beamline station (BL01B) at the National Synchrotron Radiation Laboratory (NSRL), China.

2　Results and discussion

The XRD results of as-deposited and annealed $La_2Ti_2O_7$ thin films are shown in Fig. 1. No diffraction peaks are observed for the as-deposited thin film, indicating it is amorphous. We further study the temperature-induced crystallization of these films through XRD analysis. The (0 2 0), (−1 0 4) and (− 8 1 0) diffraction peaks appear when the sample was annealed at 900℃, with the temperature being higher than the crystallization temperature of La_2O_3 (500℃)[23] and TiO_2 (800℃)[24]. This indicates that the Ti concentration is crucial for obtaining $La_2Ti_2O_7$ films with high crystallization temperatures. The diffraction peaks become stronger when increasing the annealing temperature. The crystallization of $La_2Ti_2O_7$ film is quite satisfactory when annealed at 1000℃. No other La—Ti—O phases were observed and all the peaks were attributed to the $La_2Ti_2O_7$ phase.

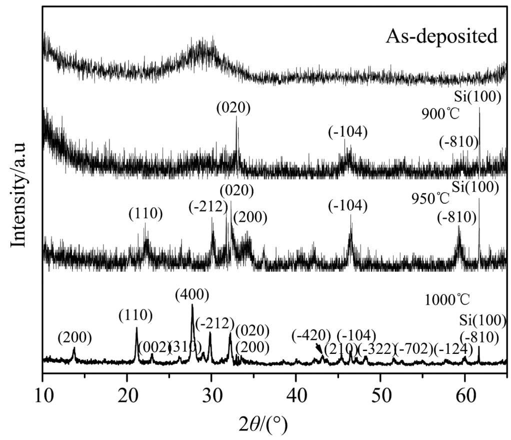

Fig.1　XRD patterns of $La_2Ti_2O_7$ films deposited on Si (100) after post-annealing at different temperatures for 30s

The surface morphology of the films was analyzed by atomic force microscopy (AFM). Fig. 2 shows the AFM images of the as-deposited and annealed $La_2Ti_2O_7$ films. The as-deposited film exhibited a surface roughness of 0.4592 nm, the surface roughness of the films clearly increased upon increasing the post-annealing temperature. The $La_2Ti_2O_7$ film annealed at 900℃ showed a smooth surface (3.862 nm), while the one annealed at 1000℃ had a rough surface (8.924 nm). We suggest that this behavior is due to an increased self-diffusion of lanthanum, titanium and oxygen during high-temperature annealing which causes an enlargement of grains, thus increasing the surface roughness of the $La_2Ti_2O_7$ film.

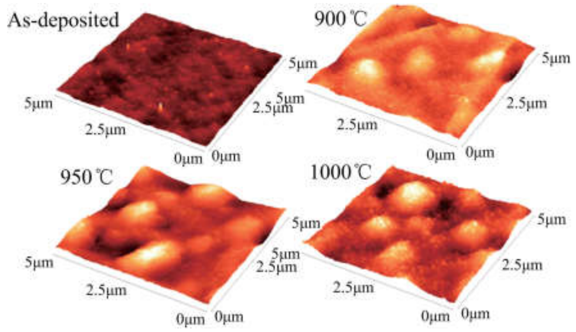

All images are taken in a 5μm by 5μm area

Fig.2 AFM images of $La_2Ti_2O_7$ films before and after post-annealing at 900℃, 950℃ and 1000℃

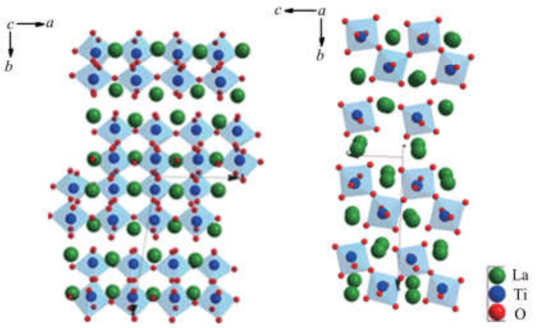

Fig.3 Schematic diagram of $La_2Ti_2O_7$ with monoclinic structure

According to the group theoretical analysis, $La_2Ti_2O_7$ is a member of a homologous series of layered structures built from (110) perovskite slabs with the generic composition $A_mB_mO_{3m+2}$ ($m=4, 5$)[25]. The schematic diagram of monoclinic $La_2Ti_2O_7$ with space group of P_{21} is shown in Fig.3. The theoretical group analysis predicts the following irreducible representations of acoustical and optical zone-center modes[26-27].

$$\Gamma = A_g + 15A_u + B_g + 15B_u$$

In these modes, A_u and B_u modes are infrared modes and the A_g, B_u modes are Roman modes.

Fig.4 shows infrared transmission spectra for as-deposited and annealed $La_2Ti_2O_7$ films. By analyzing the infrared spectra, we can get the infrared phonon modes and the contribution of each mode to the dielectric constant. For the as-deposited sample, the spectra is dominated by three broad peaks because of its amorphous structure. These bands in the 200 ~ 600 cm^{-1} region are due to Ti—O vibrations or probably, to complex motions involving the participation of both La and Ti cations. In the case of the crystalline $La_2Ti_2O_7$ samples, more phonon bands are observed and the intensity increases with increasing annealing temperature.

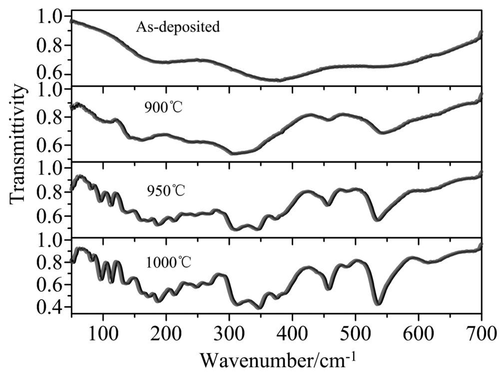

Fig.4 Infrared transmission spectra (black line) and their corresponding fitting spectra (light grey) by the classical oscillator model of the $La_2Ti_2O_7$ films at different temperatures

In order to quantitatively analyze the phonon modes. the infrared spectra were fitted with the classical Lorentz oscillator model (Eq. (1)).

$$\varepsilon^*(\omega) = \varepsilon_\infty + \sum_{j=1}^{n} \frac{S_j}{\omega_j^2 - \omega^2 + i\omega\gamma_j} \qquad (1)$$

where $\varepsilon^*(\omega)$ is the complex dielectric function, ε_∞ is the dielectric constant caused by the electronic polarization at a higher frequency, and n is the number of transverse optical vibration modes. The oscillation parameters ω_j, S_j and γ_j are the frequency, oscillator strength, and damping factor of the jth Lorentz oscillator, respectively[28-29]. The real part (ε') and imaginary part (ε'') of complex dielectric function can also be extracted from the frequency dependence of transmission data by the classical oscillator model.

The fitted spectra match well with the measured ones, as shown in Fig.4, and the fitted parameters are listed in Tab.1. The spectra were fitted by only 5 phonon modes for the as-deposited film because of the broadening of the main peaks and fitted by 22 phonon modes for the sample annealed at 1000℃. The number of modes used to fit the infrared spectra is less than that predicted by the group theory because the thin film itself loses some phonon vibration modes compared to its bulk structure, and amorphous films further lose several phonon vibration modes compared to the crystalline ones. The possible overlapping and the low intensity of some of them also lead to a reduction of the phonon modes[26].

Tab.1 D-L model fitting parameters of $La_2Ti_2O_7$ films before and after post-annealing at 900℃, 950℃ and 1000℃

As-deposited			900℃			950℃			1000℃		
$\varepsilon_0=20$　$\varepsilon_\infty=4.6$			$\varepsilon_0=34.1$　$\varepsilon_\infty=4.78$			$\varepsilon_0=40$　$\varepsilon_\infty=4.8$			$\varepsilon_0=46$　$\varepsilon_\infty=5$		
ω_{TOj}/cm^{-1}	S_j	γ_j/cm^{-1}	ω_{TOj}/cm^{-1}	S_j	γ_j/cm^{-1}	ω_{TOj}/cm^{-1}	S_j	γ_j/cm^{-1}	ω_{TOj}/cm^{-1}	S_j	γ_j/cm^{-1}
			65.71	14.6	75.9	51.3	17.94	85.03	64	19.3	87.3
									80.5	0.76	5.29
89.1	5.85	84.3	97.6	3.85	54.6	95.8	2.91	52.8	95.9	3.06	8.73
						112	1.41	5.96	112	1.74	6.67
			140	0.91	17.1	135	1.89	15.4	135	3.14	16.9
170.	4.54	102	163	5.53	56.4	166	3.91	30.5	161	2.77	19.8
									171	0.77	10.2
						188	2.59	21.7	188	4.18	24.3
211.	3.82	126	214	3.57	99.2	212	2.96	59	213	1.89	21.5
									233	0.44	17.5
						250	0.95	18	247	1.01	22.3
									267	0.76	21.5
335.	4.45	193	321	4.91	106	312	1.15	23.1	312	1.92	27.3
						340	1.24	30.4	342	1.61	28.6
						378	1.07	29.9	379	1.44	42.1
									438	0.16	26.6
			457	0.08	24.7	454	0.29	24.9	456	0.27	14.8
									485	0.11	24.7
									534	0.09	7.81
561	1.34	184	566	0.61	73.8	565	0.53	19.3	563	0.44	27.1
			619	0.21	95.6	611	1.09	281	622	0.31	85.6

The pyrochlore structure of $La_2Ti_2O_7$ may be described as the TiO_6 octahedra which are linked by their corners to form hexagonal crowns whose center is filled with the La^{3+} cations as shown in Fig.3. For the as-deposited sample, the first, third and fifth modes of the five active modes correspond to La—TiO_6 vibration at 90cm^{-1}, Ti—O_6 stretching at 210cm^{-1} and TiO_6 bending at 560cm^{-1}, respectively[30-31]. The second and forth modes at 170cm^{-1} and 370cm^{-1} respectively may be related to the T—O vibration and La—O[9]. The oscillation of the phonons becomes clearer and stronger with the rise of the annealing temperature, and it shows that the oscillation of the phonons at a low frequency have a higher oscillator strength.

We can further compare the difference of dielectric constants between the as-deposited and annealed thin films. The real part and imaginary part of dielectric functions are shown in Fig.5, and the fitting ε_0 and ε_∞ are given in Tab.1. It is noted that the high frequency dielectric constants ε_∞ of the thin films are about 4.6～5, which suggests that the large values of the static dielectric constant originates from the part of lattice component. Especially, the low frequency phonons with high oscillator strength give the main contribution to the dielectric constant. The obtained ε_0 for $La_2Ti_2O_7$ thin film annealed at 1000℃ is ～46. However, the ε_0 value decreases following the lowering of the annealing temperature, which is ～ 40 and 34.1 for the samples annealed at 950℃ and 900℃, respectively. Nevertheless, the ε_0 of annealed thin films are much larger than that of as-deposited thin films which is only ～ 20. As mentioned above, the dielectric constant is directly related to the infrared phonon mode. In annealed thin films, the lowest phonon mode around 60cm^{-1} gives above 40% contribution to the dielectric constant. However, this mode disappears in the as-deposited amorphous thin film. Meanwhile, the loss and weakness of many other phonon modes also reduce the dielectric constant of the as-deposited sample.

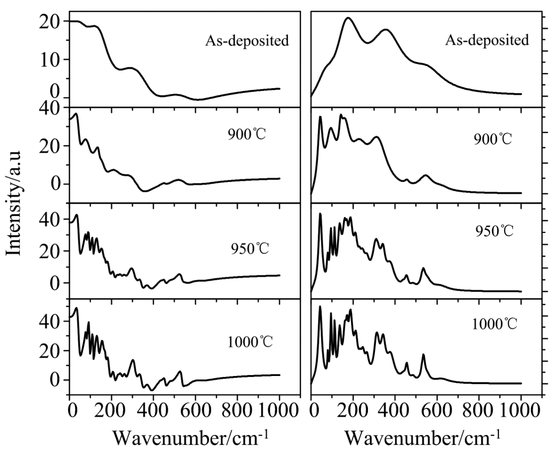

Fig.5 Real (left) and imaginary (right) parts of the dielectric function of the $La_2Ti_2O_7$ films at different temperatures

3 Conclusion

In summary, the effect of annealing on the structural properties of the $La_2Ti_2O_7$ thin films deposited on Si (100) substrates has been studied. The XRD, AFM and FT-IR data reveal that the thin film annealed at 1000℃ shows a good crystallization and a high dielectric value. The as-deposited amorphous thin film has the lowest dielectric constant because it loses some phonon modes, especially the low frequency mode. The measured thermal properties of the thin film suggest that the $La_2Ti_2O_7$ film should be a promising candidate for future high-k gate dielectrics.

References

[1] Semiconductor Industry Association. The National Technology Roadmap for Semiconductors [R]. Washington, DC: SIA, 2000.

[2] MULLER D A, SORSCH T, MOCCIO S, et al. The electronic structure at the atomic scale of ultrathin gate oxides[J]. Nature, 1999, 399(6738): 758-761.

[3] PACKAN P A. Pushing the limits[J]. Science, 1999, 285(5436): 2079-2081.

[4] DEGRAEVE R, PANGON N, KACZER B, et al. Temperature acceleration of oxide breakdown and its impact on ultra-thin gate oxide reliability [C]// Proceedings of the Symposium on VLSI Technology. Kyoto, Japan: IEEE, 1999: 59-60.

[5] RIOS R, ARORA N D. Determination of ultra-thin gate oxide thicknesses for CMOS structures using quantum effects [C]// Proceedings of the IEEE International Electron Devices Meeting. San Francisco: IEEE, 1994: 613-616.

[6] ARDEN W M. The international technology roadmap for semiconductors perspectives and challenges for the next 15 years[J]. Current Opinion in Solid State and Materials Science, 2002, 6(5): 371-377.

[7] CHATTERJEE A, RODDER M, CHEN I C. A transistor performance figure-of-merit including the effect of gate resistance and its application to scaling to sub-0.25-μm CMOS logic technologies [J]. IEEE Transactions on Electron Devices, 1998, 45(6): 1246-1252.

[8] VELLIANITIS G, APOSTOLOPOULOS G, MAVROU G, et al. MBE lanthanum-based high-*k* gate dielectrics as candidates for SiO_2 gate oxide replacement[J]. Materials Science and Engineering: B, 2004, 109(1-3): 85-88.

[9] SCAREL G, DEBERNARDI A, TSOUTSOU D, et al. Vibrational and electrical properties of hexagonal La_2O_3 films[J]. Applied Physics Letters, 2007, 91(10): 102901(1-14).

[10] WILK G D, WALLACE R M, ANTHONY J M. High-κ gate dielectrics: Current status and materials

properties considerations [J]. Journal of Applied Physics, 2001, 89(10): 5243-5275.

[11] WU Y H, CHEN S B, CHIN A, et al. High quality thermal oxide grown on high temperature formed SiGe [J]. Journal of the Electrochemical Society, 2000, 147 (5): 1962-1964.

[12] ZHAO Y, TOYAMA M, KITA K, et al. Moisture-absorption-induced permittivity deterioration and surface roughness enhancement of lanthanum oxide films on silicon[J]. Applied Physics Letters, 2006, 88 (7): 072904.

[13] DEVINE R A B. Infrared and electrical properties of amorphous sputtered $(La_xAl_{1-x})_2O_3$ films[J]. Journal of Applied Physics, 2003, 93(12): 9938.

[14] EDGE L F, SCHLOM D G, BREWER R T, et al. Suppression of subcutaneous oxidation during the deposition of amorphous lanthanum aluminate on silicon [J]. Applied Physics Letters, 2004, 84 (23): 4629.

[15] VAN DOVER R B. Amorphous lanthanide-doped TiO_X dielectric films [J]. Applied Physics Letters, 1999, 74 (20): 3041.

[16] SCHROEDER T, LUPINA G, DABROWSKI J, et al. Titanium-added praseodymium silicate high-k layers on Si(001) [J]. Applied Physics Letters, 2005, 87 (2): 022902.

[17] ZHAO Y, KITA K, KYUNO K, et al. Dielectric and electrical properties of amorphous $La_{1-x}Ta_xO_y$ films as higher-*k* gate insulators [J]. Journal of Applied Physics, 2009, 105(3): 034103.

[18] JEON S, HWANG H. Electrical and physical characteristics of $PrTi_xO_y$ for metal-oxide-semiconductor gate dielectric applications[J]. Applied Physics Letters, 2002, 81(25): 4856.

[19] ATUCHIN V V, GAVRILOVA T A, GRIVEL J C, et al. Electronic structure of layered ferroelectric high-ktitanate $La_2Ti_2O_7$[J]. Journal of Physics D: Applied Physics, 2009, 42(3): 035305.

[20] LUPINA G, SCHROEDER T, DABROWSKI J, et al. Praseodymium silicate layers with atomically abrupt interface on Si(100)[J]. Applied Physics Letters, 2005, 87(9): 092901.

[21] WANG Y, QI Z, SHAO T, et al. Infrared phonon modes and local structure of amorphous and crystalline $LaLuO_3$ thin films [J]. Journal of Alloys and Compounds, 2013, 571(37): 103-106.

[22] KAWANO H, MORII K, NAKAYAMA Y. Effects of crystallization on structural and dielectric properties of thin amorphous films of $(1-x)BaTiO_{3-x}SrTiO_3$ ($x=0-0.5$, 1.0)[J]. Journal of Applied Physics, 1993, 73 (10): 5141-5146.

[23] PISECNY P, HUSEKOVA K, FROHLICH K, et al. Growth of lanthanum oxide films for application as a gate dielectric in CMOS technology [J]. Materials Science in Semiconductor Processing, 2004, 7(4-6): 231-236.

[24] YANG W, MARINO J, MONSON A, et al. An investigation of annealing on the dielectric performance of TiO_2 thin films [J]. Semiconductor Science and Technology, 2006, 21(12): 1573-1579.

[25] LICHTENBERG F, HERRNBERGER A, WIEDENMANN K, et al. Synthesis of perovskite-related layered $A_nB_nO_{3n+2}=ABO_X$ type niobates and titanates and study of their structural, electric and magnetic properties [J]. Progress in Solid State Chemistry, 2001, 29(1): 1-70.

[26] KRISHNANKUTTY K, DAYAS K R. Synthesis and characterization of monoclinic rare earth titanates, $RE_2Ti_2O_7$ (RE = La, Pr, Nd), by a modified SHS method using inorganic activator [J]. Bulletin of Materials Science, 2008, 31(6): 907-918.

[27] BALACHANDRAN U, EROR N G. X-ray diffraction and vibrational-spectroscopy study of the structure of $La_2Ti_2O_7$[J]. Journal of Materials Research, 1989, 4 (6): 1525-1528.

[28] OGISO H, NAKANO S, NAKADA M. Far-infrared spectroscopy of Au-implanted lithium niobate ($LiNbO_3$)[J]. Nuclear Instruments and Methods in Physics Research Section B: Beam Interactions with Materials and Atoms, 2009, 267(8-9): 1579-1582.

[29] BUNDESMANN C, BUIU O, HALL S, et al. Dielectric constants and phonon modes of amorphous hafnium aluminate deposited by metal organic chemical vapor deposition[J]. Applied Physics Letters, 2007, 91(12): 121916(1-3).

[30] ZHANG J, ZHAI J, CHOU X, et al. Microwave and infrared dielectric response of tunable $Ba_{1-x}Sr_xTiO_3$ ceramics [J]. Acta Materialia, 2009, 57(15): 4491-4499.

[31] CHO S Y, YOUN H J, LEE H J, et al. Contribution of structure to temperature dependence of resonant frequency in the $(1-x)La(Zn_{1/2}Ti_{1/2})O_3 \cdot xATiO_3$ (A = Ca, Sr)[J]. Journal of the American Ceramic Society, 2001, 84(4): 753-758.